

Effect of Asymmetric Functionalized Graphene Oxide (Janus GO) on Young's Modulus and Glass Transition Temperature of PSf Ultrafiltration Membrane

Mahdi Akbari¹, Mojtaba Shariaty-Niassar^{1*}, Takeshi Matsuura² and Ahmad Fauzi Ismail³

¹Transport Phenomena & Nanotech. Lab (TPNT), School of Chemical Engineering, College of Engineering, University of Tehran, P.O. Box: 11155-4563, Tehran, Iran.

²Department of Chemical and Biological Engineering, University of Ottawa, Ottawa, Ontario, K1N 6N5, Canada.

³Advanced Membrane Technology Research Centre (AMTEC), Faculty of Chemical and Energy Engineering, Universiti Teknologi Malaysia UTM, 81310 Johor Bahru, Johor, Malaysia.

(*) Corresponding author: mshariat@ut.ac.ir

(Received: 12 August 2018 and Accepted: 06 January 2019)

Abstract

In this study, effect of asymmetric functionalized graphene oxide (Janus GO) on Young's modulus and glass transition temperature of Polysulfone (PSf) ultrafiltration membranes was investigated. The membranes were prepared via phase inversion method and GO nanosheets were dispersed in casting solution by sonication. Results showed that the Normalized Young's modulus (on the basis of neat PSf membrane Young's modulus) increased from 1 to 1.35 for neat PSf membrane compared to the membrane with 1% Janus GO nanosheets. This enhancement indicated the improvement of mechanical properties of modified membranes. Also, application of Janus GO nanosheets caused enhancement of thermal stability of modified membranes by increasing glass transition temperature to 182.97 °C compared to 180.1 °C for neat PSf membrane. These improvements were ascribed to the enhancement of dispersion and stability of Janus GO nanosheets in membranes matrix.

Keywords: Janus graphene oxide, Ultrafiltration membrane, Young's modulus, Glass transition temperature.

1. INTRODUCTION

Filtration using polymeric membranes is one of the most widely used methods in membrane separation processes [1]. With increase in the application of filtration technique (especially ultrafiltration) in various fields such as food industry [2], water and waste water treatment [3, 4], medical production [5, 6], etc., new materials and also new modification methods are required to improve polymeric membranes properties and performance. There are many methods used to enhance their properties such as blending with copolymers [7], grafting with monomers [8] and addition of nanoparticles [9].

Different nanoparticles such as SiO₂ [10], TiO₂ [11], Al₂O₃ [12] and GO [13] were used to enhance various properties of polymeric membranes specially hydrophilicity, permeate flux and anti-fouling properties. It should be considered that the application of nanoparticles for improving membrane's performance also affects its mechanical and thermal properties. This issue is very important for some applications. Among nanomaterials, GO has received great attention in recent years because of its two-dimensional structure and excellent properties [14]. GO has many covalently attached groups such as

carb-oxyl, hydroxyl, epoxy and carbonyl groups that facilitate the processing and modification [15]. Lee et al. [16] studied PSf membranes with various concentrations of GO that were prepared via phase inversion method. Their result showed that Young's modulus of PSf membranes increased with increasing GO concentration up to 1.3 wt.% but for higher concentrations, Young's modulus decreased because of agglomeration of GO at high concentrations. In another study, Ionita et al. [17] investigated mechanical and thermal performances of PSf-GO membranes. They also observed that Young's modulus of the prepared membranes was enhanced up to 1 wt. % of GO but for higher concentrations, Young's modulus significantly decreased. Similar trends were observed for thermal properties of membranes [17]. Poor performance of nanocomposites at the high concentration of GO was ascribed to the presence of GO agglomeration, which reduced the GO reinforcing effect because of poor interface interaction of GO and membrane matrix [18, 19]. Moreover, GO agglomerates caused harmful concentration of stress. Functionalization of GO is one of the proposed methods to reduce negative effects of GO agglomeration. Xu et al. [20] studied the effect of functionalization of GO with organosilane agent on mechanical properties of PVDF membranes. They compared mechanical properties of GO and functionalized GO mixed matrix membranes with 1% concentration of nanofillers. They found that functionalized GO significantly improved mechanical properties of the membrane while GO caused reduction of the mechanical strength of the membrane. They assigned this result to better interfacial interaction between functionalized GO and membrane matrix as well as better dispersion (lower agglomeration) of functionalized GO. Ryu and Shanmugaraj [21] investigated the effect of GO modification by long chain alkylamines on crystallization and

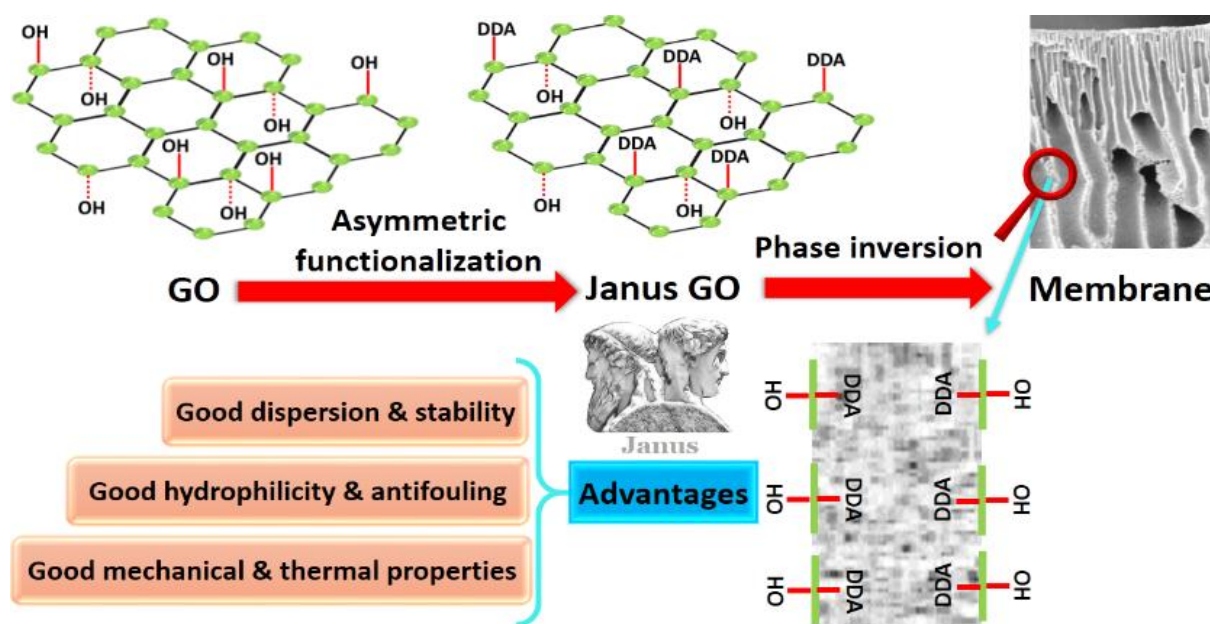
mechanical properties of isotactic polypropylene nanocomposites. Their result showed that modified GO had better dispersion and interfacial interactions with polymer that caused a significant enhancement in mechanical properties.

Since functionalization of hydrophilic nanoparticles with hydrophobic functional groups (for better dispersion and decreasing agglomeration problem) reduces their hydrophilicity, in our previous study [22], we used asymmetric functionalized GO (Janus GO) to overcome this problem. Janus GO has one hydrophilic side that contains carboxyl, hydroxyl, epoxy and carbonyl groups and also one hydrophobic side containing mainly long chain alkyl groups. In phase inversion method (for membrane preparation), hydrophobic side of Janus GO helps better dispersion and stability of nanosheets in membrane matrix, while hydrophilic side of Janus GO increases the membrane surface hydrophilicity and improves its anti-fouling properties (Figure 1). The good interaction of Janus GO with polymeric matrix not only helps to obtain better dispersion but also improves mechanical and thermal properties of the prepared membrane. Therefore, in this study, the effects of Janus GO on Young's modulus and glass transition temperature of Janus GO blended PSf membranes were investigated.

2. MATERIALS AND METHODS

2.1. Materials

Polysulfone (PSf, Udel® P-3500 LCD MB7, $M_w=77,000-83,000$, $M_n=22,000$) was procured from Solvay Specialty Polymers. Sulfuric acid (H_2SO_4), Nitric acid (HNO_3), Hydrochloric acid (HCl), Potassium permanganate ($KMnO_4$), Hydrogen peroxide (H_2O_2 , 30%), N-Methyl-2-pyrrolidinone (NMP), Paraffin (melting point=54-56°C), Dodecylamine (DDA), sodium hydroxide (NaOH) were procured from Merck. Bovine serum albumin (BSA, $M_w=68,000$ g/mol) and



graphite powder were purchased from

Sigma Aldrich.

Figure 1. Schematic of Janus GO synthesis and application in phase inversion method.

2.2. GO Preparation

Hummers' method was used to prepare GO from graphite [23]. In brief, 7 g graphite were mixed with mixture of H₂SO₄/HNO₃ (225 mL: 85 mL) at 0 °C for 1 h. Then 42 g of KMnO₄ were added slowly in 2 h to the mixture under stirring condition. Temperature of the mixture was raised to 36 °C and stirred for 2 days. After 2 days, the temperature was increased to 97 °C in 15 min. Then 1120 mL distilled water was added to the mixture and the temperature was adjusted to 30 °C. After that, 100 mL of H₂O₂ was added slowly to the mixture and stirred for 1 h. The mixture was cooled to room temperature and filtered to obtain GO, then was washed with distilled water until neutral pH. Eventually the GO was put in vacuum oven at 50 °C for 24 h.

2.3. Asymmetric Functionalization of GO

Pickering emulsion template was used for preparation of asymmetric functionalized GO (Janus GO) as described in ref [24] with some modifications. In brief, a desired amount of GO was dispersed in distilled water by sonication for 30 min in an ultrasonic bath

and then 1 h with probe ultrasonic to ensure complete dispersion. Then, the GO suspension and paraffin were put in 25 mL flask and heated to 70 °C on a heating plate and then emulsification was carried out with probe ultrasonic in pulse mode (100 W, 3 seconds on, 7 seconds off) for 1 min. The mixture was allowed to cool to room temperature and then filtered and GO-coated wax microspheres were obtained. Microspheres were sonicated for 5 min in 50 ml of NaOH aqueous solution (pH=10) to remove weakly attached GO. Then, 10 g of microspheres and 0.1 g of DDA were mixed in 60 g of aqueous ethanol solution (1/1, v/v) at 30 °C for 12 h. During reaction time, DDA reacted only with one side of GO that faces aqueous phase. To obtain Janus GO, microspheres were dissolved in chloroform and centrifuged. For further purification, Janus GO was transferred to separatory funnel and then 50 ml of distilled water was added and left for 3 days. Janus GO was collected from interface, washed with ethanol by centrifugation-sonication cycle and eventually dried in a vacuum oven at 50 °C for 1 day. For better comparison between GO and Janus GO, a same

procedure except reaction with DDA was used for some GO-coated mic-rosppheres.

2.4. Membrane Preparation

Phase inversion method was used for membranes preparation. For all samples, amount of PSf and NMP were constant (in ratio of 3 to 17) and concentration of nano-sheets was determined based on the PSf. For example for GO-0.5 membrane 0.5% of PSf was added to solution. For membrane preparation, GO or Janus GO was dispersed in NMP by sonication for 1 h. Then, PSf was added and mixture was stirred with a magnetic stirrer (100 rpm) for 12 h. To remove the bubbles the solution was further sonicated (30 min) and vacuum dried in a desiccator (1 h). The solution was cast on a glass plate by a casting knife (thickn-ess=200 μm) and after 30 seconds the cast film was immersed into coagulation bath of water at room temperature.

2.5. Characterization of Nanosheets

FESEM (model: ZEISS VP) was used for observation of GO and GO-coated micro-spheres morphology. For obtaining better results, GO was dispersed in ethanol using sonication and then deposited on a lamel. GO-coated microspheres were diluted with distilled water and then dried on the lamel. For better observation of GO nanosheets, transmission electron microscopy (TEM) was also carried out by (TEM, Philips CM30 electron microscope). EDX analysis was used to confirm the functionalization of graphene oxide nanosheets. The analysis was carried out for two samples of GO and Janus GO with the trace of oxygen, carbon and nitrogen elements using the ZEISS VP model. XRD analysis (model: Siemens D5-000) was employed with Cu $K\alpha$ radiation.

2.6. Characterization of Membrane

2.6.1. Morphology

The structure and cross-sectional morphology of the membranes were analyzed by SEM (model: ZeissDSM-960A). Samples

were cut into small parts and submerged in liquid nitrogen and fractured after 30 seconds. To enhance conductivity of the membranes, the samples were sputter-coated with gold.

2.6.2. Mechanical Strength

The mechanical strength of the membranes was characterized by the tensile strength using a universal mechanical tester (Instron, USA). The membranes were cut into a rectangular shape (1 cm \times 10cm). All the tensile tests were carried out at a stepper motor speed of 10 mm min⁻¹ at room temperature, and the average thickness of the samples was obtained from the SEM pictures. Young's modulus was calculated from the linear part of the stress-strain curve. The reported results are the averages of 3 samples.

2.6.3. Differential Scanning Calorimetry (DSC)

The glass transition temperature (T_g) is related to rigidity of the polymer chain in the membrane. T_g was obtained by differential scanning calorimetry (Mettler Toledo DSC 1) at heating rate of 10 $^{\circ}\text{C}/\text{min}$ in the range of 100–300 $^{\circ}\text{C}$ under nitrogen atmosphere.

3. RESULTS AND DISCUSSION

3.1. Characterization of Nanosheets

Figure 2 shows FESEM and TEM images of GO nanosheets. It can be observed that GO nanosheets has a layered and folded structure with a wrinkled surface.

Figure 3 exhibits XRD patterns of GO nanosheets. Graphene oxide's characteristic peak at $2\theta \sim 10^{\circ}$ was determined that is in agreement with the literature [25, 26]. The lack of other peaks shows that there are no graphite and reduced graphene oxide [26]. The EDX analysis result of GO and Janus GO are shown in Figure 4 and Table 1.

According to the results, it can be seen that the amount of carbon and nitrogen in Janus GO, rather than GO, increases while

the amount of oxygen decreases. This is due to the addition of dodecylamine to the structure of GO and also the elimination of hydroxyl group from its surface. These results together with FTIR result (in our previous study [22]) confirm the successful addition of dodecylamine to GO nanosheets.

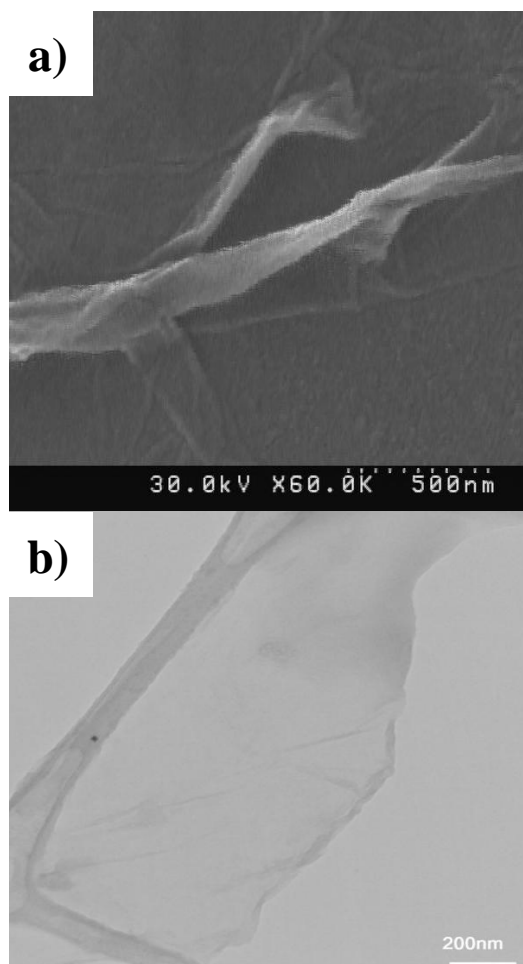


Figure 2. (a) FE-SEM and (b) TEM images of GO nanosheet.

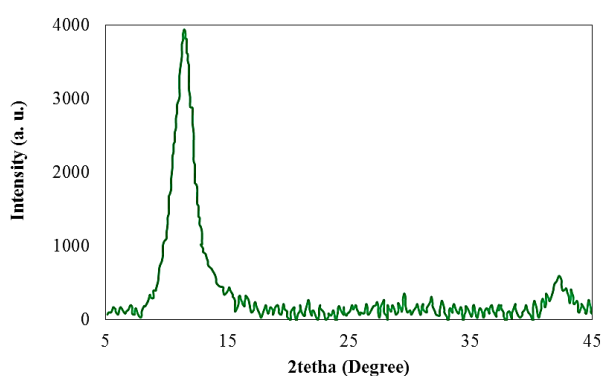


Figure 3. XRD patterns of GO.

Figure 5 a-c represent the photographs of various steps of GO-coated microspheres preparation. Figure 5 d shows FESEM image of GO-coated microspheres. As can be seen, GO nanosheets were successfully adsorbed onto the microspheres surface and stabilized them.

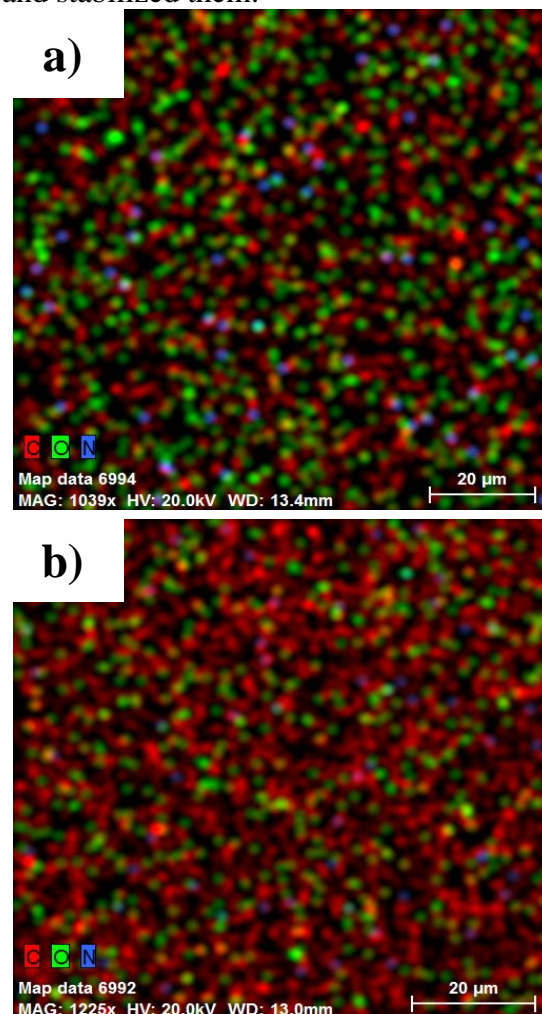


Figure 4. EDX images of (a) GO and (b) Janus GO.

3.2. Characterization of Membranes

3.2.1. Stability of GO and Janus GO Nanosheets in Casting Solution

Photographs of the casting solutions taken three months after their preparation are exhibited in Figure 9. It can be seen that GO nanosheets were precipitated at the bottom of the round bottom flask caused by their agglomeration but for Janus GO nanosheets, precipitation is hardly observable. Different behavior of GO and Janus GO may be due to their

different thickness [27, 28] and steric stabilization of Janus GO (because of DDA).

3.2.2. Morphology of Membranes

Figure 7 shows a typical SEM image of the prepared membranes. It can be seen

that the prepared membrane has a typical asymmetric porous structure with a dense skin layer

and a support layer with a finger-like structure.

Table 1. Elemental analysis of GO and Janus GO.

Sample	Normalized atomic percentage			Normalized weight percentage		
	Nitrogen	Oxygen	Carbon	Nitrogen	Oxygen	Carbon
GO	2.52	36.34	61.14	2.62	43.03	54.35
Janus GO	5.78	21.24	72.98	6.24	20.26	67.56

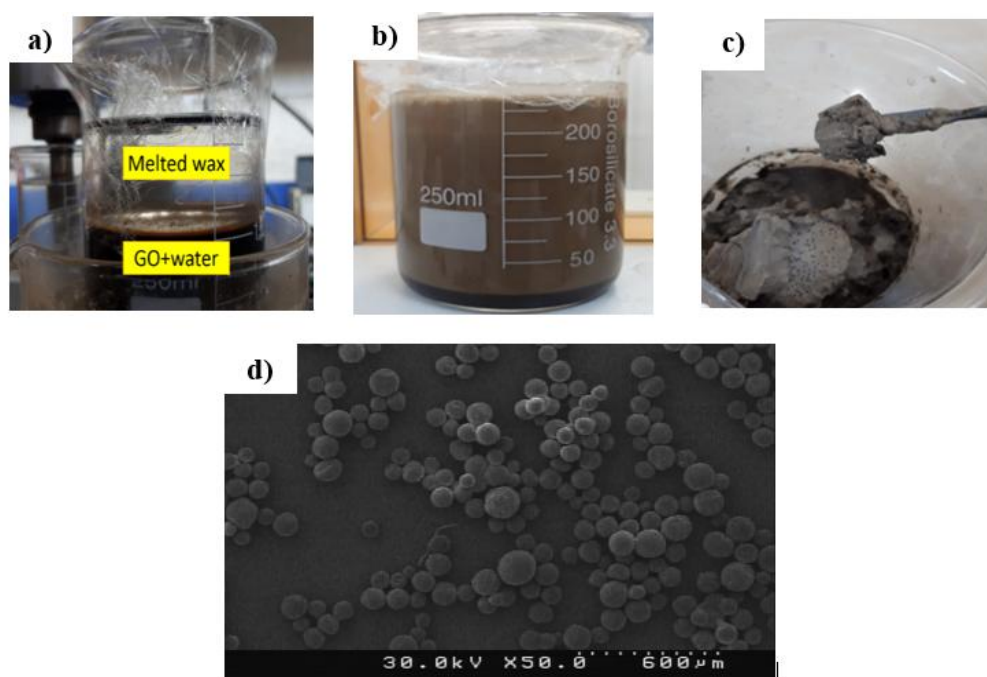


Figure 5. Photograph of melted wax and GO dispersed water before sonication (a), photograph of melted wax and GO dispersed water after sonication (b), photograph of separated microspheres (c), FESEM image of GO-coated microspheres (d).

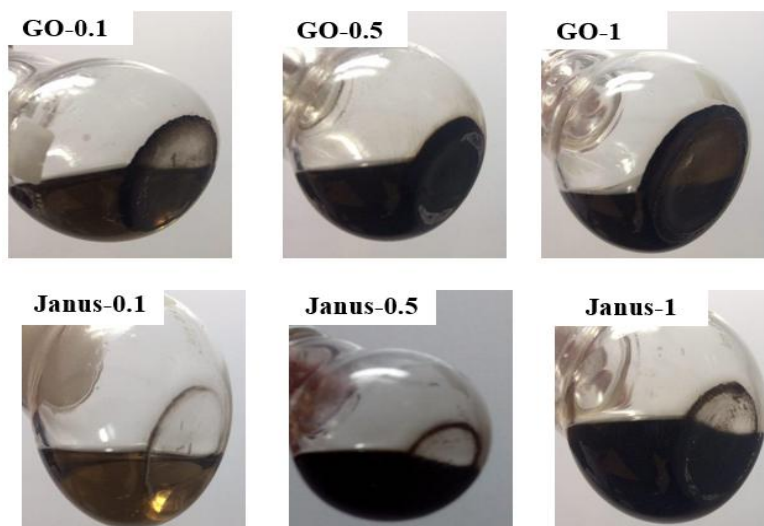


Figure 6. Photographs of casting solutions after three months of their preparation.

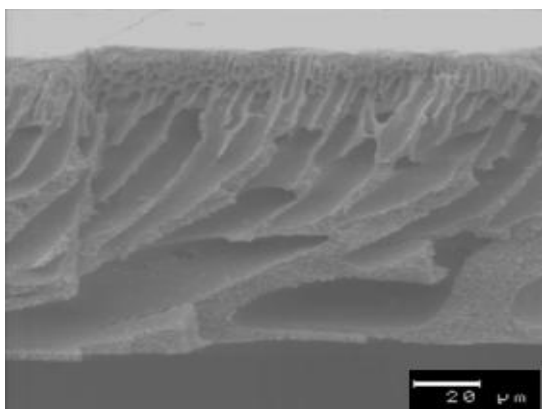


Figure 7. Typical Cross sectional SEM image of prepared membranes.

3.2.3. Mechanical Properties

Mechanical properties of blended membranes are very important for their applications [29]. Figure 8 shows the normalized Young's modulus of the prepared membranes. In the figure, normalized Young's modulus of the GO membrane increases linearly from PSf to GO-0.5. This increment can be related to the very high aspect ratio of GO nanosheets [16] and their acting as a bridge between two PSf polymer chains (30). However, further addition of GO to GO-1.0 reduced normalized Young's modulus, caused by the agglomeration of GO nanoparticles. The observed trend is in agreement with the work of Lee et al. and Ionita et al. [16, 17]. On the other hand, Young's modulus of Janus GO incorporated membranes keeps increasing linearly as the Janus nanoparticle loading increases. This is again due to the better dispersion of Janus GO nanoparticles than GO nanoparticles.

3.2.4. DSC

DSC results of PSf, GO-0.5 and Janus-1 membranes are shown in Figure 9. The results demonstrate that glass transition temperatures (T_g) of PSf, GO-0.5 and Janus-1 membranes are 180.1 °C, 181.51 °C and 182.97 °C, respectively. The strong additive-polymer interfacial interaction hinders the mobility of the surrounding

polymer segments, leading to the increase in T_g [29]. Thus, the higher T_g of the Janus-1 membrane again implies the good Janus GO nanoparticle-polymer interaction, which also enabled the improvement in the dispersion of nanoparticles.

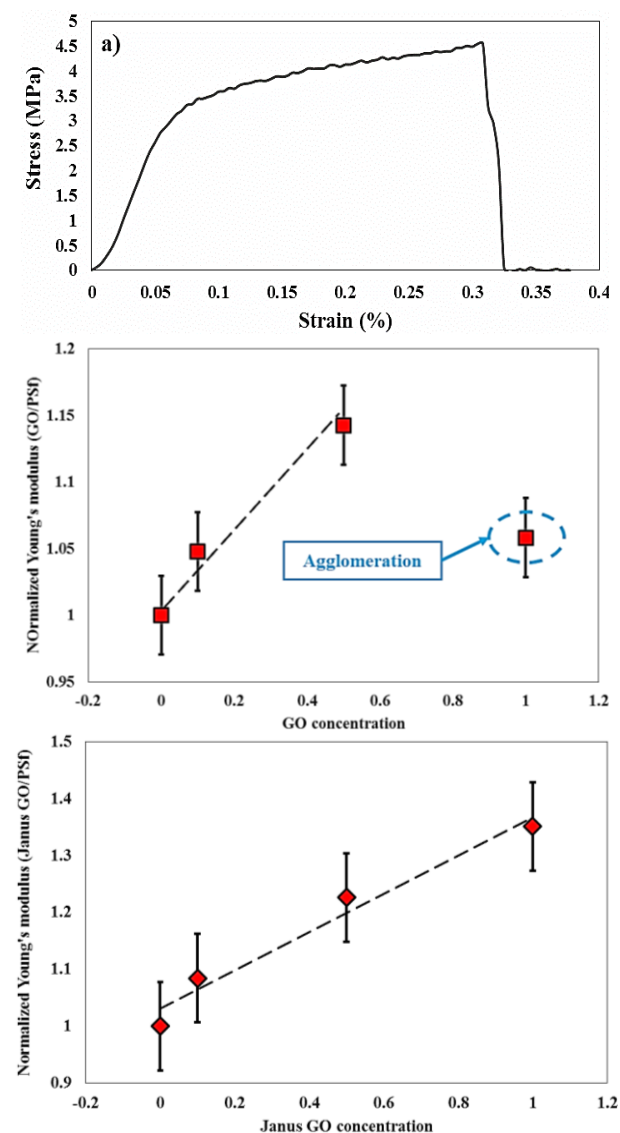


Figure 8. (a) Typical stress–strain curves of prepared membranes, (b) Normalized Young's modulus of GO blended membranes, (c) normalized Young's modulus of Janus GO blended membranes.

4. CONCLUSION

Effects of Janus GO on the Young's modulus and T_g of PSf membranes

prepared via phase inversion method were investigated. The mechanical strength and thermal stability of Janus-1 membrane were improved. Better mechanical and thermal properties of the modified membranes were ascribed to the better interaction of Janus GO and membrane matrix at interface and also better dispersion (more stability against agglomeration) of Janus GO nanosheets.

5. ACKNOWLEDGEMENT

The authors are thankful to Iran National Science Foundation (INSF) for funding this research under contract number 92013505.

REFERENCE

1. Asci, Y. S., Dramur, U., Bilgin, M., (2017). "Investigation of the separation of carboxylic acids from aqueous solutions using a pilot scale membrane unit", *J. Mol. Liq.*, 248: 391-398.
2. Conidi, C., Cassano, A., Caiazzo, F., Drioli, E., (2017). "Separation and purification of phenolic compounds from pomegranate juice by ultrafiltration and nanofiltration membranes", *J. Food. Eng.*, 195: 1-13.
3. Wei, X., Fei, Y., Shi, Y., Chen, J., Lv, B., Chen, Y., Xiang, H., (2016). "Hemocompatibility and ultrafiltration performance of PAN membranes surface-modified by hyperbranched polyesters", *Polym. Advan. Technol.*, 27(12): 1569-76.
4. Ghaee, A., Shariaty-Niassar, M., Barzin, J., Ismail, A. F., (2013). "Chitosan/polyethersulfone composite nanofiltration membrane for industrial wastewater treatment", *International Journal of Nanoscience and Nanotechnology.*, 9(4): 213-220.
5. Anisimov, S. I., Anisimova, S. Y., Baldin, A. A., Baldina, E. G., Luzanov, V. A., Denisenko, O. O., (2010). "Ultrafiltration of Cellulose Solutions for Medical Purposes Using Track Membranes", *Biomed. Eng.*, 44(4): 130-133.
6. Bhunia, T. (2018). "Different PVA-hydroxypropyl guar gum irradiated nanosilica composite membranes for model drug delivery device", *International Journal of Nanoscience and Nanotechnology.*, 14(3): 187-95.
7. Chen, S. H., Willis, C., Shull, K. R., (2017). "Water transport and mechanical response of block copolymer ion-exchange membranes for water purification", *J. Membrane. Sci.*, 544(Supplement C): 388-96.
8. Pu, Y., Huang, X., Yang, P., Zhou, Y., Xuan, S., Zhang, Y., (2017). "Effect of non-sulfonated diamine monomer on branched sulfonated polyimide membrane for vanadium redox flow battery application", *Electrochim. Acta.*, 241(Supplement C): 50-62.
9. Gul, S., Rehan, Z. A., Khan, S. A., Akhtar, K., Khan, M. A., Khan, M. I., Rashid, M. I., Asiri, A. M., Khan, S. B., (2017). "Antibacterial PES-CA-Ag₂O nanocomposite supported Cu nanoparticles membrane toward ultrafiltration, BSA rejection and reduction of nitrophenol", *J. Mol. Liq.*, 230(Supplement C): 616-624.
10. Rakhshan, N., Pakizeh, M., (2015). "The effect of chemical modification of SiO₂ nanoparticles on the nanofiltration characteristics of polyamide membrane", *Korean J. Chem. Eng.*, 32(12): 2524-2533.

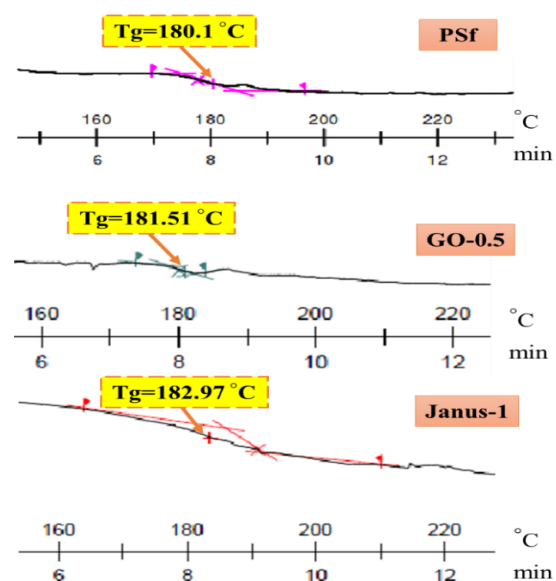


Figure 9. DSC results of PSf, GO-0.5 and Janus-1.

11. Safarpour, M., Vatanpour, V., Khataee, A., (2016). "Preparation and characterization of graphene oxide/TiO₂ blended PES nanofiltration membrane with improved antifouling and separation performance", *Desalination*, 393: 65-78.
12. Dong, H., Xiao, K. j., Li, X. l., Ren, Y., Guo, S. y., (2013). "Preparation of PVDF/Al₂O₃ hybrid membrane via the sol-gel process and characterization of the hybrid membrane", *Desalin. Water. Treat.*, 51(19-21): 3685-3690.
13. Bano, S., Mahmood, A., Kim, S. J., Lee, K. H., (2015). "Graphene oxide modified polyamide nanofiltration membrane with improved flux and antifouling properties", *J. Mater. Chem. A.*, 3(5): 2065-2071.
14. Pan T. Y., Chan, J. X., Chung, T. S., Weber, M., Staudt, C., Maletzko, C., (2015). "Simultaneously covalent and ionic bridging towards antifouling of GO-embedded nanocomposite hollow fiber membranes", *J. Mater. Chem. A.*, 3(19): 10573-10584.
15. Yang, M., Zhao, C., Zhang, S., Li, P., Hou, D., (2017). "Preparation of graphene oxide modified poly(m-phenylene isophthalamide) nanofiltration membrane with improved water flux and antifouling property", *Appl. Surf. Sci.*, 394(Supplement C): 149-159.
16. Lee, J., Chae, H. R., Won, Y. J., Lee, K., Lee, C. H., Lee, H. H., Kim, I. C., Lee, J. M., (2013). "Graphene oxide nanoplatelets composite membrane with hydrophilic and antifouling properties for wastewater treatment", *J. Membrane. Sci.*, 448: 223-230.
17. Ionita, M., Pandlele, A. M., Crica, L., Pilan, L., (2014). "Improving the thermal and mechanical properties of polysulfone by incorporation of graphene oxide", *Compos. Part. B: Eng.*, 59: 133-139.
18. Shukla, A. K., Alam, J., Alhoshan, M., Dass, L. A., Muthumareeswaran, M., (2017). "Development of a nanocomposite ultrafiltration membrane based on polyphenylsulfone blended with graphene oxide", *Sci. Rep-UK.*, 7: 41976.
19. Zhao, Y., Lu, J., Liu, X., Wang, Y., Lin, J., Peng, N., Li, J., Zhao, F., (2016). "Performance enhancement of polyvinyl chloride ultrafiltration membrane modified with graphene oxide". *J. Colloid. Interf. Sci.*, 480: 1-8.
20. Xu, Z., Zhang, J., Shan, M., Li, Y., Li, B., Niu, J., Zhou, B., Qian, X., (2014) "Organosilane-functionalized graphene oxide for enhanced antifouling and mechanical properties of polyvinylidene fluoride ultrafiltration membranes", *J. Membrane. Sci.*, 458: 1-13.
21. Ryu, S. H., Shanmugaraj, A. M., (2014). "Influence of long-chain alkylamine-modified graphene oxide on the crystallization, mechanical and electrical properties of isotactic polypropylene nanocomposites", *Chem. Eng. J.*, 244: 552-560.
22. Akbari, M., Shariaty-Niassar, M., Matsuura, T., Ismail, A. F., (2018). "Janus graphene oxide nanosheet: A promising additive for enhancement of polymeric membranes performance prepared via phase inversion", *J. Colloid. Interf. Sci.*, 527: 10-24.
23. Hummers J. r. W. S., Offeman R. E., (1958). "Preparation of graphitic oxide", *J. Am. Chem. Soc.*, 80(6): 1339-1339.
24. Wu, H., Yi, W., Chen, Z., Wang, H., Du, Q., (2015). "Janus graphene oxide nanosheets prepared via Pickering emulsion template". *Carbon.*, 93: 473-483.
25. Marcano, D. C., Kosynkin, D. V., Berlin, J. M., Sinitskii, A., Sun, Z., Slesarev, A., Alemany, L. B., Lu, W., Tour, J. M., (2010). "Improved synthesis of graphene oxide", *Acs. Nano.*, 4(8): 4806-4814.
26. Zhang, L., Liang, J., Huang, Y., Ma, Y., Wang, Y., Chen, Y., (2009). "Size-controlled synthesis of graphene oxide sheets on a large scale using chemical exfoliation", *Carbon.*, 47(14): 3365-3368.
27. Tang, Y. P., Paul, D. R., Chung, T. S., (2014). "Free-standing graphene oxide thin films assembled by a pressurized ultrafiltration method for dehydration of ethanol", *J. Membrane. Sci.*, 458: 199-208.

28. Yu, Z., Zhang, S., Gao, J., Chung, T. S., (2016). "Layer-by-layer construction of graphene oxide (GO) framework composite membranes for highly efficient heavy metal removal", *J. Membrane. Sci.*, 515: 230-237.
29. Cai, N., Li, C., Luo, X., Xue, Y., Shen, L., Yu, F., (2016). "A strategy for improving mechanical properties of composite nanofibers through surface functionalization of fillers with hyperbranched polyglycerol", *J. Mater. Sci.*, 51(2): 797-808.
30. Mukherjee, R., Bhunia, P., De, S., (2016). "Impact of graphene oxide on removal of heavy metals using mixed matrix membrane", *Chem. Eng. J.*, 292: 284-297.